Rip current evidence by hydrodynamic simulations, bathymetric surveys and UAV observation

Guido Benassai[1], Pietro Aucelli[2], Giorgio Budillon[2], Massimo De Stefano[2], Diana Di Luccio[2], Gianluigi Di Paola[2], Raffaele Montella[2], Luigi Mucerino[3], Mario Sica[4], and Micla Pennetta[5]

[1]Department of Engineering, University of Naples Parthenope
[2]Department of Science and Technology, University of Naples Parthenope
[3]Department of Earth, Environment and Life Sciences, University of Genova
[4]Autorità di Bacino Campania Centrale
[5]Department of Earth, Environment and Resources Sciences, University of Naples Federico II

Correspondence to: Guido Benassai (guido.benassai@uniparthenope.it)

Abstract. The prediction of the formation, spacing and location of rip currents is a scientific challenge that can be achieved by means of different complementary methods. In this paper the analysis of numerical and experimental data, including RPAS (Remotely Piloted Aircraft Systems) observations, allowed to detect the presence of rip currents and rip channels at the mouth of Sele river, in the Gulf of Salerno, southern Italy. The dataset used to analyze these phenomena consisted of two different bathymetric surveys, a detailed sediment analysis and a set of high-resolution wave numerical simulations, completed with Google Earth[TM] images and RPAS observations. The grain size trend analysis and the numerical simulations allowed to identify the rip current occurrence, forced by topographically constrained channels incised on the seabed, which were compared with observations.

Keywords: rip-currents, hydrodynamic simulations, transport vectors, UAV observation.

1 Introduction

The monitoring and the forecasting of beach processes become particularly critical along the unstable coastal areas, possibly subjected to coastal vulnerability (Di Paola et al. (2014)), and coastal risk due to sea level rise (Benassai et al. (2015)) and subsidence (Aucelli et al. (2016)). The evolution of winds, waves and wind-driven sea circulation is of great applicative relevance for the observation of oceanographic phenomena (Bidlot et al. (2002)). The offshore wind-wave simulations are accomplished by observations obtained by satellite images, by active satellite-based microwave Synthetic Aperture Radar (SAR) (Benassai et al. (2012b, 2013, 2012a)), while the coastline monitoring can be surveyed by remote sensing acquisition (Nunziata et al. (2016, 2014)), or at shorter time scale can be observed by RPAS (Remotely Piloted Aircraft Systems) and video monitoring system (Casella et al. (2014)). A possible feedback between these wave-driven circulations, sediment processes and beach morphology is the occurrence of rip currents.

Rip currents are narrow, intense seaward flowing jets that originate within the surf zone and broaden outside the breaking zone. The alongshore variation of wave height fuels modification of wave-induced momentum flux or radiation stress (Longuet-

Higgins and Stewart (1964)), which cross-shore gradient is balanced by the hydrostatic pressure, giving rise to wave set-up on the beach. The longitudinal gradient of set-up generates local longshore currents which concentrate and join up to generate an offshore return flow which forms the rip current. This gradient can be caused by alongshore differences of incident wavefield due to wave groups (Dalrymple (1975)), wave-current interactions (Dalrymple and Lozano (1978)), or wavefield interaction

5   with edge waves (Symonds and Ranasinghe (2001)).

Comprehensive rip current observations require bathymetry measurements, directional wave records, tide and current detection. Alternatively, wave climate can be simulated with high-resolution numerical models in order to obtain the rip current spacing, which is comparable with their wavelength. With regard to bathymetry, rip channels have found to be quasi-periodic alongshore perturbations which occur at the observed alongshore spacing *O(100m)* (MacMahan et al. (2006)), when the waves

10 approach at near normal incidence (Bowen (1969)).

With regard to tides, rip currents have long been observed to vary with the tide elevation, in particular they are tidally modulated, such that a decrease in tidal elevation leads to an increase of rip current flow to a relative maximum (Sonu (1972); MacMahan et al. (2005)), linking the danger of rip currents to lower tidal elevations (Engle (2002)).

These strong offshore directed currents are the cause of the majority of fatalities within the beach environment (Drozdzewski

15 et al. (2012); Brander et al. (2013); Brighton et al. (2013); Zhang et al. (2012)). Therefore, many attempts have been made to relate the rip current morphology to the local wave climate, shoreline orientation, sediment size and tidal conditions. Due to a number of laboratory and field investigations, possible rip-current occurrence was associated to simple parameters that can be easily evaluated with few data and field measurements. The earliest studies of rip currents paid attention to the relationship between rip current spacing and the surf zone width (Shepard and Inman (1950)). Other authors (Short and Brander

20 (1999); Sasaki et al. (1977)) demonstrated that the rip spacing y_r is directly related to the dimensionless fall velocity parameter introduced by Wright and Short (1984) to classify beach states (from dissipative to reflective):

$$\Omega = \frac{H}{T w_s} \tag{1}$$

in which H is the breaker height, T is the incident wave period and w_s is the mean sediment fall velocity (Dean et al. (1973)). The intermediate beach states (Ω=2-5) are characterized by rip current occurrence.

25 In this paper we investigated the rip current spacing and morphology with numerical and experimental methods, including RPAS observations which have been already used for topographic mapping (Turner et al. (2016)), and recently extended their applicability to the surf zone characterization (Holman et al. (2017)). In order to establish a correlation between beach morphology and the rip current features, the fall velocity parameter was related to rip spacing in the coastal area at the Sele River mouth in the Gulf of Salerno, which was the subject of coastal vulnerability and risk evaluation (Di Paola et al. (2011);

30 Benassai et al. (2012a, 2014)) and of coastal morphodynamics (Pennetta et al. (2011b)). The index Ω was constructed with the grain size diameter on different transects, together with wave conditions obtained by numerical simulations. The validation of rip current occurrence associated with the reference Ω range was supported by Google Earth[TM] products (orthophoto) obtained in 2007, 2013 and 2015 and more recent images obtained by an RPAS survey. The final goal was assesses the reliability of Ω to represent an index of rip-current occurrence.

These preliminary results can be used in an operational model chain context starting from the forecasted wind till offshore and nearshore wave conditions leading to rip-currents. In this case, the RPAS model chain validation can be crucial to detect dangerous rip current conditions associated with Ω index.

This paper is structured as follows: the study area, with its morphological and climatological features, is introduced in section 2. The data and models are described in section 3. Numerical and field results are presented and discussed in section 4. Discussion and conclusion are finally drawn in sections 5, 6 respectively.

2 Study area and wave climate

The study concerns a stretch of the beach which borders seawards the alluvial plain of the Sele River, one of the widest alluvial coastal plains of central-southern Italy. This plain stretches between the high rocky coasts of Amalfi, to the NW, and Cilento promontory to the SE, (Campania) and is limited towards the sea by a narrow sandy beach which extends from NW to SE in the Gulf of Salerno, in the southern Tyrrhenian Sea (Fig. 1). The plain represents the emerged portion of a morpho-tectonic depression related to the opening of the Tyrrhenian ocean basin, started during the Upper Miocene (Bartole et al. (1984); Casciello et al. (2006); Aucelli et al. (2012)).

The presence of beach-dune ridges, located in the outer portion of the plain, marks the sea level highstands and Upper Pleistocene paleo-coastlines. During the Holocene, three phases of sandy coastal ridges interrupted the progradational trend of the coastline, with discontinuous dune system height about 3m a.s.l. (Fig. 1a). This dune system can be considered as a natural barrier to sea ingression (e.g. Pennetta et al. (2011a); Pappone et al. (2012); Amato et al. (2013)). Moreover the back-ridge depressions, recently drained, are localized in several and large areas, with a mean elevation of 0.50/1.5m a.s.l. (Pappone et al. (2011)). During the last century, the Sele coastline was affected by erosion which was strong around the main river mouths, due to numerous hydraulic dams which reduced the sediment supply. Nowadays, the coast is rather stable and only the Sele mouth zone is in erosion (Alberico et al. (2012)). The wave climate was obtained by a directional waverider wave buoy (40°27'26.4"N, 14°51'41.16"E) installed and managed by the Provincial Authority in the Bay of Salerno on approx. 35 meter deep water, for 2014-2016 years. The directional distribution of the significant wave heights, consisting of 32024 samples (Fig. 1b), is in close agreement with the one obtained by the longer data set of the offshore buoy of Ponza (Piscopia et al. (2002)). Figure 1c gives the same directional distribution for significant wave heights $H_s \geq 2$m. Finally, the histogram in Fig. 1d shows the cumulated H_s occurrence frequency for each direction, confirming that the wave directions associated with the most frequent waves are mainly SW (about 56%) and WSW (about 22%).

3 Data and models

3.1 Bathymetric and sediment surveys

In order to define a detailed mapping of emerged and submerged beach, we performed two bathymetric surveys along 155 transects spaced by 100 meters, from the dune till 10m depth. The emerged beach profile were surveyed using a Differential
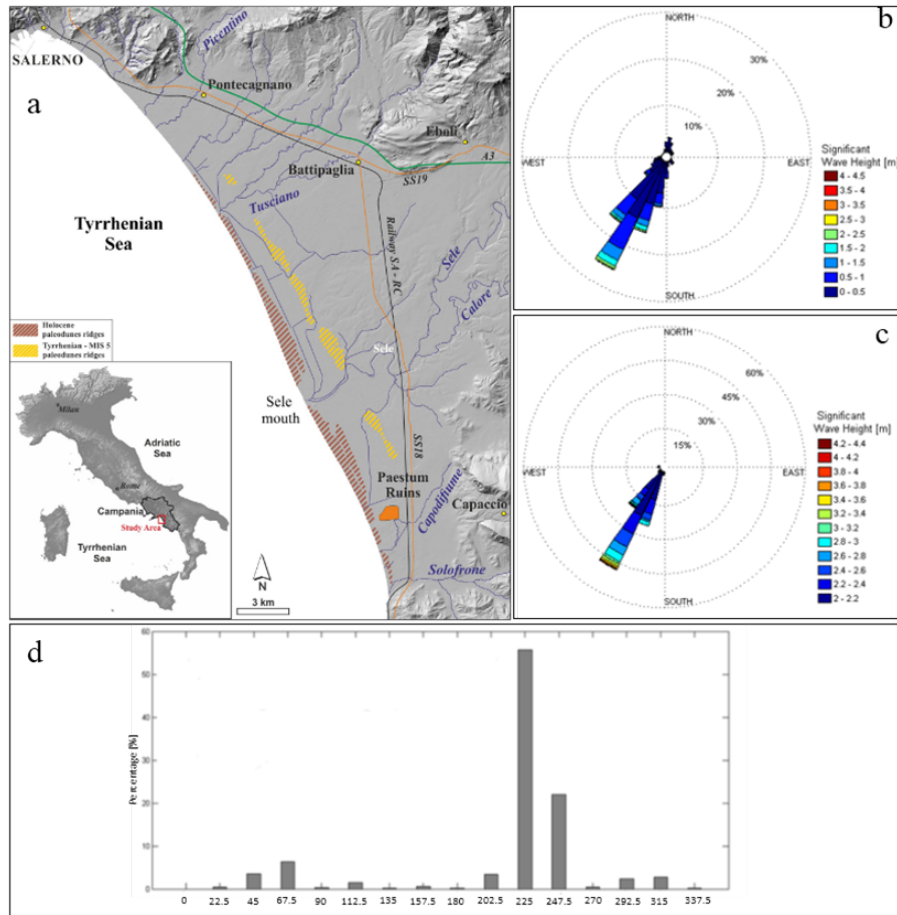
Figure 1. Location map of Coastal Sele Plain (a); directional distribution of the H_s (b) and of the $H_s \geq 2m$ recorded by Salerno buoy in the 2014-2016 years (c); H_s occurrence probability [%] for each direction (d).

Global Position System (DGPS), while the submerged beach profiles were recorded using the interferometric sonar SEA SWATH plus 468 kHz integrated with a single beam system and a GPS RTK dual frequency navigation system. These data were included in a geographic information system (GIS) framework to generate a DTM (*Digital Terrain Model*), from which the isobaths needed for detecting rip channels and bars were extracted, with a point density of two meters along each transect.

5   In order to determine the sediment mean size, during the first survey 280 sediment samples were collected, 120 of them in the submerged beach using a Van Veen grab sampler. The analysis of grain size distribution with the Graphic method (Folk and Ward (1957)) was applied, in order to relate the sediment data to morphological ones obtained in other coastal areas (De Pippo et al. (2003); Pennetta et al. (2016); Mangoni et al. (2016)).

3.2 Sediment dynamical analysis

Submerged beach sediments grain size (ϕ) was collected, air-dried (temperature of 105-110°C), and sieved (set of silks arranged in mechanical stirrer at intervals of 1/2 ϕ) in accordance with the American Society for Testing and Materials Method D422 (ASTM D422). For each sample, we extract the statistical parameter in accordance to Folk and Ward (1957). This statistical analysis is based on occurrence frequencies identification related to the most prevalent grain size classes (mode of the grain size distribution), defined as "modal classes", of a single sediment sample. Contours of the modal iso-density were plotted by assigning the proper percentage values of the average modal formula (related to the different modal subpopulations) to sediments samples map points positions. Trend vectors are defined comparing the grain size parameters of each sample with its neighbour, identified on the basis of a characteristic distance that represents the space scale of sampling. Those vectors summarize, in terms of movement directions, the sediment dynamics on the submerged beach of the studied area.

3.3 Wave simulation and hydrodynamic model

In order to simulate the offshore wave features in Gulf of Salerno and propagate them on the coastline, we used a scientific workflow (Giunta et al. (2005)) implemented by the *Campania Center for Marine and Atmospheric Monitoring and Modelling* (CCMMMA) hosted by the University of Naples "*Parthenope*", using a high performance computing (HPC) system (Montella et al. (2011); Di Lauro et al. (2012)) for simulation and open environmental data dissemination (Montella et al. (2007)). The weather/sea forecasting tool has been configured using an HPC infrastructure to manage and run a modeling system based on the algorithms implemented in the open-source numerical models *Weather Research and Forecasting* (WRF) (Skamarock et al. (2001) and *WaveWatchIII* (WWIII) (Tolman et al. (2009)) organized in a workflow (Pham et al. (2012)). The operational configuration is based on the WRF numerical model which gives the atmospheric forcing (10 meters wind fields) needed to estimate the offshore waves. Wave simulations were carried out using the *WaveWatch* III, a third generation wave model developed at NOAA/NCEP. Preliminary implementation and validation for simulating the wave propagation along the Campania Region coastline (Gulf of Naples) were conducted by Benassai and Ascione (2006). Subsequently WRF and WWIII models were coupled in an operational configuration for realtime applications, using also a high resolution bathymetry, to simulate extreme weather coastal floodings along the coast of the municipality of Naples. The WWIII model domain has been configured with 350x200 grid points and 0.01° spatial resolution in latitude (Lat_{min}=39.50N, Lat_{max}=41.49N) and in longitude (Lon_{min}=12.50E, Lon_{max}=15.99E), covering the South Tyrrhenian Sea. WWIII model outputs include gridded fields with the associated significant wave heights (H_s), periods (T_m), directions (Dir) and relative spectral informations.

The offshore wave model outputs were the forcing of the 2D near-shore model XBeach (Roelvink et al. (2009)). This is a two-dimensional model for wave propagation, long waves and mean flow, sediment transport and morphological beach changes during storms. XBeach concurrently solves the time-dependent short wave action balance, roller energy equations, nonlinear shallow water equations of mass and momentum, sediment transport formulations and the bed update on the scale of wave groups. In the Netherlands, a rip current prediction model system was used on the basis of bathymetry measurement through the application application of the XBeach hydrodynamic model (Roelvink et al. (2009)). In this paper XBeach was used to con-

firm, through hydrodynamic simulations, the occurrence of bathymetric rips evidence by the rip channels previously identified. For this purpose, the model was run with the offshore wave conditions identified in the month of February 2008, obtained by the WWIII wave model. The computational grid has generated merging field data collected in 2008 and the deeper bathymetry, from 10m to 40m depth, supplied by the Istituto Idrografico della Marina Italiana. An irregular mesh was used to obtain a

5   higher resolution across the surf zone and a lower resolution far from the coast. The size of the elements was about 5m on the beach and 25m off the coast. The wave conditions at the offshore boundary were inserted using the JONSWAP spectrum module using the wave condition supplied by WWIII model for rip currents events highlighted by sediment transport vectors in 2008.

3.4 RPAS survey

10   Remotely piloted aerial vehicles used for scientific or research activities, are defined RPAS and are subjected to the regulations of the Italian Navigation Code, in accordance with the Italian Civil Aviation Authority (ENAC) Regulation Issue n. 2 (2015). This Regulation provides safety levels for different kinds of operations. The Regulation classifies the RPAS according to their weight (take-off mass lower or higher than 25 kg) and classifies operations according to their criticality. In our survey, the operations are defined VLOS (Visual Line of Sight) because the remote pilot maintains continuous visual contact with the

15   aerial vehicle. VLOS operations are permitted in daylight, up to a maximum height of 150 m above ground level, within a maximum horizontal distance of 500 m. Our beach survey was defined "non critical" because it consisted in VLOS operations which do not overfly, even in case of malfunction and/or failures: i) congested areas, gathering of persons, urban areas; ii) critical infrastructures.

In order to perform rip current observations (Fig. 2a, b, c) we used an RPAS hexacopter which weighed about 2500g, carried

20   on board a GPS, a multi-directional accelerometer and a remote flight control. The max height and max radius (vertical and horizontal distance between the aircraft and the home point) were set to the default value of 2000m. The hovering accuracy was ±0.8m in vertical and ±2.5m in horizontal, while the max ascent and descent speed were 6 m/s and 4.5 m/s, respectively. A failsafe function system was activated if the connection between the multirotor and the remote control was accidentally disconnected during flight, which provided fly back to the point of take-off and land automatically. The RPAS was equipped

25   with a Canon ELPH 130 camera with 16 Mpixel (4608 by 3456 pixels) sensor because of its lightweight, manual functions, and programming capabilities through open source custom software.

In order to generate orthophotos from the acquired RPAS photos, we used the Z-Map software produced by MENCI, allowed to correct and eliminate radial-distortion, relief distortion, tilt and pitch of aircraft, and scale variations caused by changes in altitude along the flight lines. Therefore, by means of this methodology an orthophoto of the area has been obtained with a

30   root mean square error (RMSE) of ±1 m. The ortho-rectified aerial images has been georeferenced using ground control points (GCP) measured at the ground altitude using the Trimble R6 DGPS (Differential Global Positioning System) in RTK (Real Time Kinematic) mode, a differential GNSS technique which provides high positioning performance in the proximity of a base station (FISC-35 LAT=40°46'13.74"; LON.= 14°47'24.91" (http://it.smartnet-eu.com)). As targets points for DGPS we used

Figure 2. RPAS on flight on the surveyed beach.

some fixed structures and 25 mobile targets (rectangular red card 297mm×240mm) placed on the berm terrace for the time of the survey.

4 Results

4.1 Sediment analysis and morphodynamics

5   Comparison of different profiles is used to make morphodynamic characterization on the study area. The bathymetric difference between DTM recorded in February and September 2008 was mapped with a resolution of 5x5 m^2, with the areas suffering from a bathymetric drop of more than 0.1m (reduction of sediment volumes), the ones characterized by a bathymetric lifting of more than 0.1m (increased sediment volumes) and the areas remaining substantially in equilibrium, with the difference in height between -0.1m and +0.1m (Fig. 3a, with the detail north of the Sele mouth in Fig. 3b). The comparison between the

10   two morphological structures derived from the different bathymetric surveys showed the formation of transverse channels to the coast, engraved at the bottom, probably generated by rip currents. These channels are developed mainly between 0 and 5 meters affecting the bars, in origin parallel to the shore, fragmenting them into smaller sand bars, transverse to the shoreline. The bars are constituted by fine and relatively unsorted sands. The increased size of the sediment in the channels as well as its higher sorter correlates well with the high hydrodynamic energy of flowing water in the channels modeled by rip currents.

15   ### 4.2 Hydrodynamics

The results of the offshore wave numerical simulations and propagation on shoaling waters have been used to establish the inshore wave conditions which are responsible for the sediment transport behaviour. In particular, the waves coming offshore from WSW, which occur with almost 20% percentage, due to a significant clockwise rotation in the shoaling zone, giving rise to waves almost normal to the bathymetry. The wave normal incidence is responsible for the coastal cell circulation and

20   the associated rip currents (Fig. 4a). The waves coming offshore from SW, which occur with almost 58% also show a similar behaviour, giving rise to the same cell circulation. Nevertheless, the frequency distributions of the highest waves shows the more significant influence of the western waves, which are susceptible to generate an almost longshore transport coming from
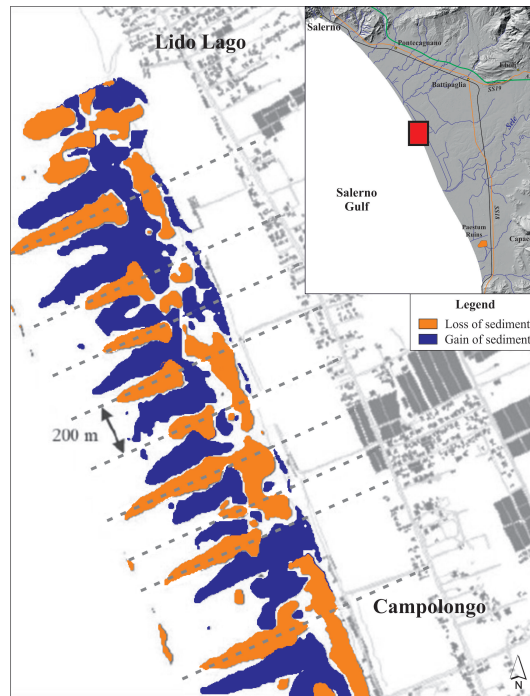
Figure 3. Loss and gain of sediment volumes in the north of the Sele mouth (modified from Pennetta et al. (2011b)). The dotted lines representing the rip channels identifying the most probable position of the rip currents.
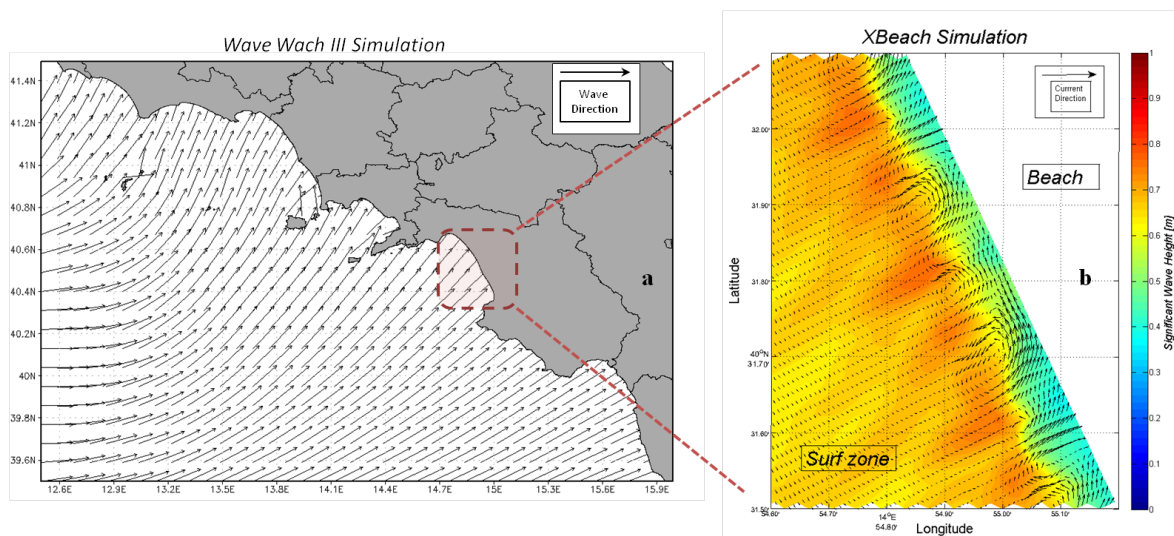
Figure 4. Offshore wave simulation associated with bathymetric survey of February 2008 with wave direction coming from WSW (a); Hydrodynamic wave simulation giving rise to rip current formation (b)).

NW.

The XBeach model output reproduced the rip currents analysed with sediment transport vectors (Fig. 4b). The results describe the wave height incidence and the flow direction simulated by XBeach model, at 16:00 PM of February 2, 2008. In particular, four rip-current cells are evident in the simulations, as well as a significant current flow directed towards offshore the rip spacing which is consistent with the results obtained by the bathymetric comparison. Moreover, the results show the rotation of the flow close to the coastline during the time step considered, and the decrease of the wave height in the rip neck in comparison with the feeder current zone. These results show that the rip current flows do not occur during extreme events, rather confirm that they occur when the significant wave height (H_s) values are between 0.5m and 1m, with mean wave periods (T_m) between 4 and 6 seconds. The simulations also put the emphasis on the fact that cell circulation is driven by longshore gradients in wave set-up and beach morphology.

4.3 Transport trends

The procedure proposed by Gao and Collins (1994) defined trend vectors for the 120 sampling considered. According to this procedure, five grain size trends were associated with net transport directions, reported in table 1 together with their percentage of occurrence. Coarse sand (SP2) with a frequency of 21.76%, Medium sand (SP3) with a frequency of occurrence of 25.45%, Fine sand (SP4) with a frequency of occurrence 20.08% and Very Fine Sand (SP5) with a frequency of occurrence of 30.66%, were the most statistically significant classes for the sediment transport vectors identification. The first was allocated more or less in a uniform way, between foreshore and the depth of -2m, the second showed a spot pattern between foreshore and the depth of -3m. The third is confined to a wide zone of the submerged beach, the last one is located all over the submerged beach with a modal frequency gradient following the bathymetry patterns towards the open sea (according to the typical behaviour of the lower grain size particles). This very fine sand modal fraction SP5 was mostly associated with the rip currents, evidenced by well-defined sediment transport vectors patterns, with moving directions (perpendicular to the shoreline) towards the open sea (Fig. 5a). The modal subpopulation SP4 (Fine Sand), showed a more complex coastal dynamics (Fig. 5b). This grain size fraction seemed to move, driven by rip currents, towards open sea only within the -3/-4m depths, then the sediments have shown to rotate and run parallel to the shoreline mainly South-eastwards, driven by longshore currents.

4.4 Google Earth[TM] products and RPAS survey

The rip current features obtained by the hydrodynamic and sediment calculations were compared with the ones observed by Google Earth[TM] (Fig. 6a,b,c) and RPAS images (Fig. 7a,b,c,d,e). corresponding with the sea states characteristics reported in table 2. The comparison between the simulated and remotely observed sea states evidences that the simulated sea states coming from W correspond to the ones observed on 28/06/2007 and 02/05/2013 (Fig. 6a, b), while the ones coming from WSW correspond to the sea states observed on 29/05/2015 (Fig. 6c). Finally, the RPAS observed rip currents are associated with sea states being characterized by longer swell mixed with sea waves generated by wind directions coming from land. This residual swell coming from W and SW is still capable of giving rise to low-defined rip currents, as shown in Fig. 7. These qualitative results are confirmed by the values of the non-dimensional fall velocity Ω given for each transect and for

Table 1. Frequency distribution for each modal class of the sample

	Modal class	Size range [mm]	Modal peak [mm]	Frequency [%]
SP1	GRAVEL	19.214-2.378	2.378	2.06
SP2	COARSE SAND	0.802 -0.595	0.595	21.76
SP3	MEDIUM SAND	0.296-0.254	0.294	25.45
SP4	FINE SAND	0.250-0.210	0.213	20.08
SP5	VERY FINE SAND	0.105-0.101	0.102	30.66
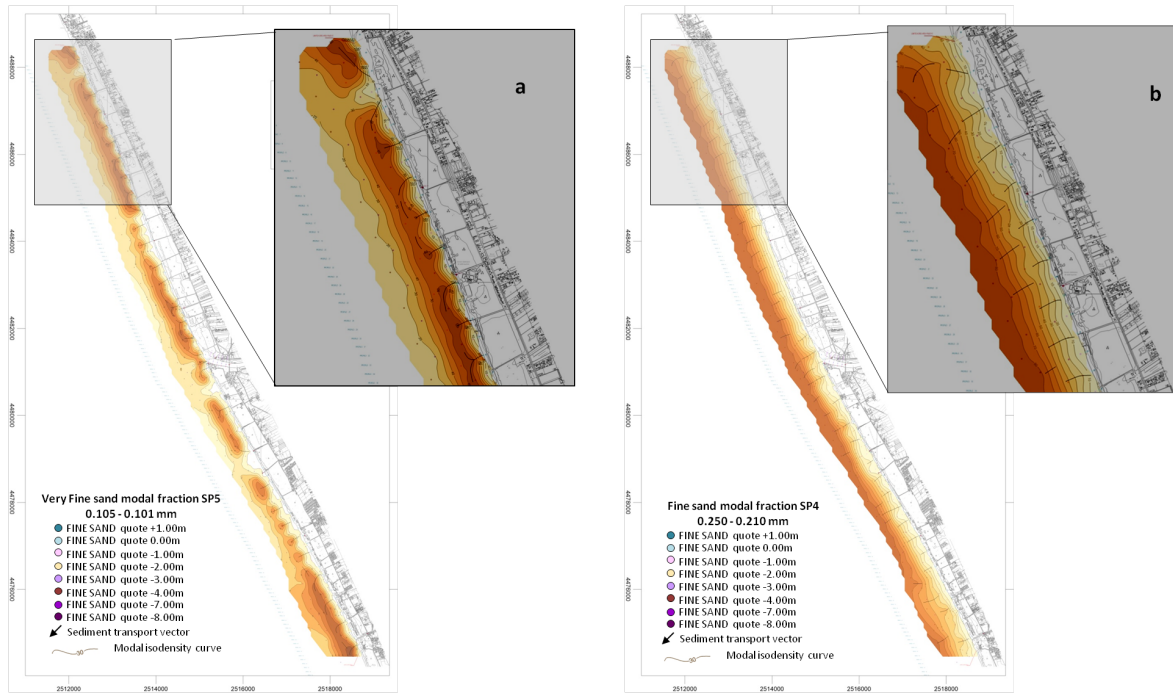
Figure 5. Sediment transport vectors for the whole area referred to the modal subpopulation SP5-Very Fine Sand (a) and SP4-Fine Sand(b).

each observed period in the histogram of Fig. 8. The results show clearly that i) the mean Ω values are quite different for well defined rip-currents observed cases and low defined rips cases and ii) the mean Ω values associated with 2013 and 2015 sea states (well defined rip-currents) are included in the range reported by Castelle et al. (2010), while the Ω values associated with the other cases (2007 and 2017) are outside of this range.

Figure 6. Evidence of rip-currents in Google Earth[TM] images a) 28/06/2007 (Image©2016 European Space Imaging); b) 02/05/2013 (Image©2016 Digital Globe); c) 29/05/2015 (Image Landsat/Copernicus).

Table 2. Wave characteristics during numerical simulations and remote observations

	28/06/2007	02/02/2008	02/05/2013	29/05/2015	21/01/2017
H_s [m]	1.46	0.91	0.33	0.46	0.67
T_m [sec]	5.8	4.11	2.99	3.47	2.71
Dir [°N]	275.10	228.29	284.23	206.20	14.83

5   Discussion

The comparison of different profiles and wave numerical simulations in the shallow coastal area of the Sele mouth in the Gulf of Salerno (Southern Italy) identified the features of the nearshore circulation, which often produced rip currents. The hydrodynamic inshore simulations clearly identified the cell circulation associated with the shore-normal wave propagation evidenced by the WWIII model. These hydrodynamic results agree with the sediment transport trends, which evidenced that the class of fine sand is brought into suspension in a wide zone of the submerged beach between the -2m and -7m bathymetry, giving rise to rip currents for the first 2-3m depth, then being distributed by the longshore coastal dynamics. The rip spacing of few hundred meters obtained by the bathymetric, sediment and hydrodynamic analysis is in accordance with observations in the range of the dimensionless fall velocity parameter Ω=2-5.

6   Conclusions

In this paper the rip current morphodynamics on a micro-tidal beach addressed by means of hydrodynamic and sediment dynamics modelling was validated by Google Earth[TM] and RPAS observations. The wave numerical simulations identified the occurrence of a rip current cell circulation in restricted ranges of heights, periods and incident directions. These hydrodynamic
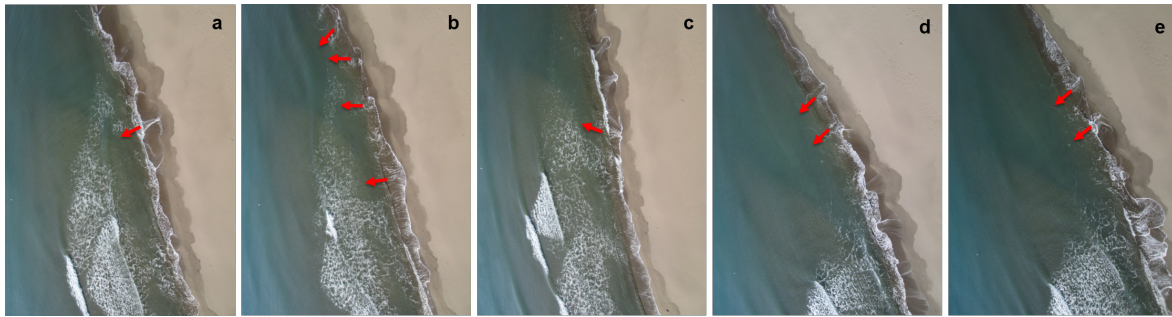
Figure 7. Evidence of rip-currents during RPAS acquisition in individual images captured on 21/01/2017. The red arrows are representative of the rip-currents.
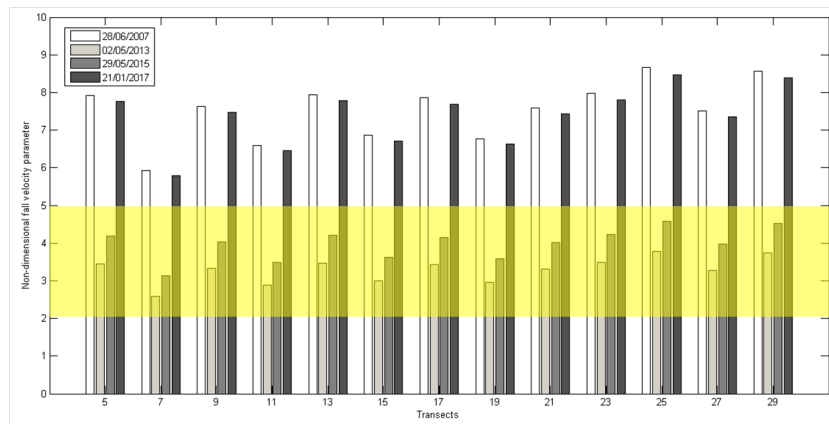
Figure 8. Histogram of the Ω values of each transect. The yellow strip is the range mostly associated with rip currents (Castelle et al. (2010)).

conditions, together with the sediment characteristics, were related with the non-dimensional fall velocity parameter, which proved to be an efficient index for the rip current formation. In fact, the remote observations of well-defined rips performed by Google Earth$^{\text{TM}}$ and RPAS images confirmed the rip current occurrence in a restricted Ω range. The present results can be used as a basis for a beach hazard forecasting system in order to enhance the swimmers safety. As a matter of fact, the observed channel rips are quite stationary over several days in this long stretch of coastline, giving rise to persistent danger in the surf zone.

Acknowledgements. The authors are grateful to the CCMMMA (*Centro Campano per il Monitoraggio e la Modellistica Marina e Atmosferica*, http://meteo.uniparthenope.it) that is the forecast service of the University of Napoli "*Parthenope*" for the real time monitoring and forecast of marine, weather and air quality conditions in the Mediterranean area, with a specific focus on the Campania Region. The CCMMMA provided the hardware and software resources for the offshore numerical simulations. Additional thanks are addressed to the

C.U.G.RI. (*Inter-University Consortium for the Prediction and Prevention of Major Hazards*), to the Civil Protection Department of the Campania Region which provided the Salerno wave buoy data, and to Dr. Caira who provided the RPAS survey on the coastal area.

References

Alberico, I., Amato, V., Aucelli, P., D'argenio, B., Di Paola, G., and Pappone, G.: Historical shoreline change of the Sele Plain (Southern Italy): The 1870–2009 time window, Journal of Coastal Research, 28, 1638–1647, doi:10.2112/JCOASTRES-D-10-00197.1, 2012.

Amato, V., Aucelli, P., Ciampo, G., Cinque, A., Di Donato, V., Pappone, G., Petrosino, P., Romano, P., Rosskopf, C., and Ermolli, E. R.: Relative sea level changes and paleogeographical evolution of the southern Sele plain (Italy) during the Holocene, Quaternary International, 288, 112–128, doi:10.1016/j.quaint.2012.02.003, 2013.

Aucelli, P. P., Amato, V., Budillon, F., Senatore, M. R., Amodio, S., D'Amico, C., Da Prato, S., Ferraro, L., Pappone, G., and Ermolli, E. R.: Evolution of the Sele River coastal plain (southern Italy) during the Late Quaternary by inland and offshore stratigraphical analyses, Rendiconti Lincei, 23, 81–102, doi:10.1007/s12210-012-0165-5, 2012.

Aucelli, P. P. C., Di Paola, G., Incontri, P., Rizzo, A., Vilardo, G., Benassai, G., Buonocore, B., and Pappone, G.: Coastal inundation risk assessment due to subsidence and sea level rise in a Mediterranean alluvial plain (Volturno coastal plain–southern Italy), Estuarine, Coastal and Shelf Science, 2016.

Bartole, R., Savelli, D., Tramontana, M., and Wezel, F.-C.: Structural and sedimentary features in the Tyrrhenian margin off Campania, Southern Italy, Marine Geology, 55, 163–180, doi:10.1016/0025-3227(84)90067-7, 1984.

Benassai, G. and Ascione, I.: Implementation and validation of WaveWatchIII model offshore the coastlines of Southern Italy, in: 25th International Conference on Offshore Mechanics and Arctic Engineering, pp. 553–560, American Society of Mechanical Engineers, doi:10.1115/OMAE2006-92555, 2006.

Benassai, G., Di Paola, G., Aucelli, P., and Maffucci, A.: The response of Sele coastal plain to storm impacts, Rend Online Soc Geol Italy, 21, 474–476, 2012a.

Benassai, G., Migliaccio, M., Montuori, A., Ricchi, A., et al.: Wave Simulations Through Sar Cosmo-Skymed Wind Retrieval and Verification with Buoy Data, in: The Twenty-second International Offshore and Polar Engineering Conference, International Society of Offshore and Polar Engineers, 2012b.

Benassai, G., Migliaccio, M., and Montuori, A.: Sea wave numerical simulations with COSMO-SkyMed© SAR data, Journal of Coastal Research, 65, 660–665, 2013.

Benassai, G., Di Paola, G., Aucelli, P., Passarella, M., and Mucerino, L.: An inter-comparison of coastal vulnerability assessment methods, in: Engineering Geology for Society and Territory-Volume 4, pp. 45–49, Springer, 2014.

Benassai, G., Di Paola, G., and Aucelli, P.: Coastal risk assessment of a micro-tidal littoral plain in response to sea level rise, Ocean & Coastal Management, 104, 22–35, doi:10.1016/j.ocecoaman.2014.11.015, 2015.

Bidlot, J.-R., Holmes, D. J., Wittmann, P. A., Lalbeharry, R., and Chen, H. S.: Intercomparison of the performance of operational ocean wave forecasting systems with buoy data, Weather and Forecasting, 17, 287–310, 2002.

Bowen, A. J.: Rip currents: 1. Theoretical investigations, Journal of Geophysical Research, 74, 5467–5478, doi:10.1029/JC074i023p05467, 1969.

Brander, R., Dominey-Howes, D., Champion, C., Del Vecchio, O., and Brighton, B.: Brief communication: a new perspective on the Australian rip current hazard, Natural hazards and earth system sciences, 13, 1687, doi:10.5194/nhess-13-1687-2013, 2013.

Brighton, B., Sherker, S., Brander, R., Thompson, M., and Bradstreet, A.: Rip current related drowning deaths and rescues in Australia 2004-2011, Natural hazards and earth system sciences, 13, 1069, doi:10.5194/nhess-13-1069-2013, 2013.

Casciello, E., Cesarano, M., and Pappone, G.: Extensional detachment faulting on the Tyrrhenian margin of the southern Apennines contractional belt (Italy), Journal of the Geological Society, 163, 617–629, doi:10.1144/0016-764905-054, 2006.

Casella, E., Rovere, A., Pedroncini, A., Mucerino, L., Casella, M., Cusati, L. A., Vacchi, M., Ferrari, M., and Firpo, M.: Study of wave runup using numerical models and low-altitude aerial photogrammetry: A tool for coastal management, Estuarine, Coastal and Shelf Science, 149, 160–167, 2014.

Castelle, B., Michallet, H., Marieu, V., Leckler, F., Dubardier, B., Lambert, A., Berni, C., Bonneton, P., Barthelemy, E., and Bouchette, F.: Laboratory experiment on rip current circulations over a moveable bed: Drifter measurements, Journal of Geophysical Research: Oceans, 115, doi:10.1029/2010JC006343, 2010.

Dalrymple, R. A.: A mechanism for rip current generation on an open coast, Journal of Geophysical Research, 80, 3485–3487, 1975.

Dalrymple, R. A. and Lozano, C. J.: Wave-current interaction models for rip currents, Journal of Geophysical Research: Oceans, 83, 6063–6071, 1978.

De Pippo, T., Donadio, C., and Pennetta, M.: Morphological control on sediment dispersal along the southern Tyrrhenian coastal zones (Italy), Geol Rom, 37, 113–121, 2003.

Dean, R. G. et al.: Heuristic models of sand transport in the surf zone, in: First Australian Conference on Coastal Engineering, 1973: Engineering Dynamics of the Coastal Zone, p. 215, Institution of Engineers, Australia, 1973.

Di Lauro, R., Giannone, F., Ambrosio, L., and Montella, R.: Virtualizing general purpose GPUs for high performance cloud computing: an application to a fluid simulator, in: 2012 IEEE 10th International Symposium on Parallel and Distributed Processing with Applications, pp. 863–864, IEEE, doi:10.1109/ISPA.2012.136, 2012.

Di Paola, G., Iglesias, J., Rodríguez, G., Benassai, G., Aucelli, P., and Pappone, G.: Estimating coastal vulnerability in a meso-tidal beach by means of quantitative and semi-quantitative methodologies, Journal of Coastal Research, pp. 303–308, doi:10.2112/SI61-001.30, 2011.

Di Paola, G., Aucelli, P. P., Benassai, G., and Rodríguez, G.: Coastal vulnerability to wave storms of Sele littoral plain (southern Italy), Natural hazards, 71, 1795–1819, doi:10.1007/s11069-013-0980-8, 2014.

Drozdzewski, D., Shaw, W., Dominey-Howes, D., Brander, R., Walton, T., Gero, A., Sherker, S., Goff, J., and Edwick, B.: Surveying rip current survivors: preliminary insights into the experiences of being caught in rip currents, Natural Hazards and Earth System Sciences, 12, 1201, doi:10.5194/nhess-12-1201-2012, 2012.

Engle, J.: Formulation of a Rip Current Predictive Index Using Rescue Data Jason Engle*, James MacMahan, Robert J. Thieke, Daniel M Hanes and Robert G Dean* Graduate Assistant, Department of Civil and Coastal Engineering, University of Florida Phone:(352) 392-9537 ext-1410; Email: engle@ coastal. ufl. edu, in: 2002 National Conference on Beach Preservation Technology. Florida Shore & Beach Preservation Association, p. 285, 2002.

Folk, R. L. and Ward, W. C.: Brazos River bar: a study in the significance of grain size parameters, Journal of Sedimentary Research, 27, 1957.

Gao, S. and Collins, M.: Analysis of grain size trends, for defining sediment transport pathways in marine environments, Journal of Coastal Research, pp. 70–78, 1994.

Giunta, G., Montella, R., Mariani, P., and Riccio, A.: Modeling and computational issues for air/water quality problems: A grid computing approach, Nuovo Cimento C Geophysics Space Physics C, 28, 215, doi:10.1393/ncc/i2005-10184-3, 2005.

Holman, R. A., Brodie, K. L., and Spore, N. J.: Surf Zone Characterization Using a Small Quadcopter: Technical Issues and Procedures, IEEE Transactions on Geoscience and Remote Sensing, doi:10.1109/TGRS.2016.2635120, 2017.

Longuet-Higgins, M. S. and Stewart, R.: Radiation stresses in water waves; a physical discussion, with applications, in: Deep Sea Research and Oceanographic Abstracts, vol. 11, pp. 529–562, Elsevier, doi:10.1016/0011-7471(64)90001-4, 1964.

MacMahan, J., Thornton, E., Stanton, T., and Reniers, A.: RIPEX—rip currents on a shore-connected shoal beach, Marine Geology, 218, 113–134, 2005.

5 MacMahan, J. H., Thornton, E. B., and Reniers, A. J.: Rip current review, Coastal Engineering, 53, 191–208, doi:10.1016/j.coastaleng.2005.10.009, 2006.

Mangoni, O., Aiello, G., Balbi, S., Barra, D., Bolinesi, F., Donadio, C., Ferrara, L., Guida, M., Parisi, R., Pennetta, M., et al.: A multidisciplinary approach for the characterization of the coastal marine ecosystems of Monte Di Procida (Campania, Italy), Marine Pollution Bulletin, 112, 443–451, doi:10.1016/j.marpolbul.2016.07.008, 2016.

10 Montella, R., Giunta, G., and Riccio, A.: Using grid computing based components in on demand environmental data delivery, in: Proceedings of the second workshop on Use of P2P, GRID and agents for the development of content networks, pp. 81–86, ACM, doi:10.1145/1272980.1272995, 2007.

Montella, R., Coviello, G., Giunta, G., Laccetti, G., Isaila, F., and Blas, J. G.: A general-purpose virtualization service for HPC on cloud computing: an application to GPUs, in: International Conference on Parallel Processing and Applied Mathematics, pp. 740–749, Springer,
15 doi:10.1007/978-3-642-31464-3_75, 2011.

Nunziata, F., Migliaccio, M., Li, X., and Ding, X.: Coastline extraction using dual-polarimetric COSMO-SkyMed PingPong mode SAR data, IEEE Geoscience and Remote Sensing Letters, 11, 104–108, 2014.

Nunziata, F., Buono, A., Migliaccio, M., and Benassai, G.: Dual-polarimetric C-and X-band SAR data for coastline extraction, IEEE Journal of Selected Topics in Applied Earth Observations and Remote Sensing, 9, 4921–4928, 2016.

20 Pappone, G., Alberico, I., Amato, V., Aucelli, P., and Di Paola, G.: Recent evolution and the present-day conditions of the Campanian Coastal plains (South Italy): the case history of the Sele River Coastal plain, WIT Trans Ecol Environ, 149, 15–27, doi:10.2495&CP110021, 2011.

Pappone, G., Aucelli, P. P. C., Aberico, I., Amato, V., Antonioli, F., Cesarano, M., Di Paola, G., and Pelosi, N.: Relative sea-level rise and marine erosion and inundation in the Sele river coastal plain (Southern Italy): scenarios for the next century, Rendiconti Lincei, 23, 121–129, doi:10.1007/s12210-012-0166-4, 2012.

25 Pennetta, M., Corbelli, V., Esposito, P., Gattullo, V., and Nappi, R.: Environmental Impact of Coastal Dunes in the Area Located to the Left of the Garigliano River Mouth (Campany, Italy)., Journal of Coastal Research, pp. 421–427, doi:10.2112/SI61-001.52, 2011a.

Pennetta, M., Sica, M., and Abbundo, R.: Canali da rip currents nella spiaggia sommersa presso la foce del Fiume Sele (Golfo di Salerno, Italia), in: Congresso annualeGEOSED, pp. 27–28, doi:10.3301/ROL.2011.42, 2011b.

Pennetta, M., Brancato, V. M., De Muro, S., Gioia, D., Kalb, C., Stanislao, C., Valente, A., and Donadio, C.: Morpho-sedimentary features
30 and sediment transport model of the submerged beach of the 'Pineta della foce del Garigliano'SCI Site (Caserta, southern Italy), Journal of Maps, 12, 139–146, doi:10.1080/17445647.2016.1171804, 2016.

Pham, Q., Malik, T., Foster, I. T., Di Lauro, R., and Montella, R.: SOLE: Linking Research Papers with Science Objects, in: IPAW, pp. 203–208, Springer, doi:10.1007/978-3-642-34222-6, 2012.

Piscopia, R., Inghilesi, R., Panizzo, A., Corsini, S., and Franco, L.: Analysis of 12-year wave measurements by the Italian Wave Network,
35 in: 28° ICCE Conference, pp. 121–133, 2002.

Roelvink, D., Reniers, A., Van Dongeren, A., de Vries, J. v. T., McCall, R., and Lescinski, J.: Modelling storm impacts on beaches, dunes and barrier islands, Coastal engineering, 56, 1133–1152, doi:10.1016/j.coastaleng.2009.08.006, 2009.

Sasaki, T., Horikawa, K., and Hotta, S.: Nearshore current on a gently sloping beach, in: Coastal Engineering 1976, pp. 626–644, 1977.

Shepard, F. and Inman, D.: Nearshore circulation, in: Proc. of First Coastal Engineering Conference, pp. 50–59, 1950.

Short, A. D. and Brander, R. W.: Regional variations in rip density, Journal of Coastal Research, pp. 813–822, 1999.

Skamarock, W. C., Klemp, J. B., and Dudhia, J.: Prototypes for the WRF (Weather Research and Forecasting) model, in: Preprints, Ninth Conf. Mesoscale Processes, J11–J15, Amer. Meteorol. Soc., Fort Lauderdale, FL, 2001.

5 Sonu, C. J.: Field observation of nearshore circulation and meandering currents, Journal of Geophysical Research, 77, 3232–3247, 1972.

Symonds, G. and Ranasinghe, R.: On the formation of rip currents on a plane beach, in: Coastal Engineering 2000, pp. 468–481, 2001.

Tolman, H. L. et al.: User manual and system documentation of WAVEWATCH III TM version 3.14, Technical note, MMAB Contribution, 276, 220, 2009.

Turner, I. L., Harley, M. D., and Drummond, C. D.: UAVs for coastal surveying, Coastal Engineering, 114, 19–24, 2016.

10 Zhang, Z., Li, N., Xie, W., Liu, Y., Feng, J., Chen, X., and Liu, L.: Assessment of ripple effect and spatial heterogeneity of total losses in the capital of China after a great catastrophe shocks, Natural hazards and earth system sciences, doi:10.5194/nhess-17-367-2017, 2012.